MINISTRY OF EDUCATION AND TRAINING
VIETNAM ACADEMY OF SCIENCE AND TECHNOLOGY

GRADUATE UNIVERSITY OF SCIENCE AND TECHNOLOGY

NGUYEN TRUNG HUY

STUDY ON FABRICATION AND CHARACTERIZATION OF HIGH-BREAKDOWN VOLTAGE VARISTOR CERAMICS BASED ON NANO-ZnO AND OXIDE ADDITIVES

SUMMARY OF DISSERTATION ON SCIENCES OF MATTER

Major: Electronic Materials

Code: 9 44 01 23

Ha Noi – 2026

The dissertation is completed at: Graduate University of Science and Technology, Vietnam Academy Science and Technology

Supervisors:

Supervisor 1: Dr. Do Quang Tham, Institute of Materials Science - Vietnam Academy of Science and Technology

Supervisor 2: Dr. Nguyen Thi Thu Trang, Institute of Materials Science - Vietnam Academy of Science and Technology

Referee 1: ………………………………………………………………….

Referee 2: ………………………………………………………………….

Referee 3: ………………………………………………………………….

The dissertation is examined by Examination Board of Graduate University of Science and Technology, Vietnam Academy of Science and Technology at …………………………….(time, date, month, year)

The dissertation can be found at:

1. Graduate University of Science and Technology Library
2. National Library of Vietnam

INTRODUCTION

Overvoltage caused by lightning strikes and switching operations is a major threat to electrical power systems, resulting in equipment failure, insulation breakdown, and power interruptions. Vietnam experiences approximately 6.9 million lightning strikes annually (about 20 strikes/km^2/year), making the development of effective overvoltage protection materials essential for improving power system reliability.

Among existing protection technologies, Zinc Oxide (ZnO)-based metal oxide varistors (MOVs) are widely used because of their excellent non-linear electrical characteristics. When the applied voltage exceeds a threshold value, ZnO varistors rapidly switch from a high-resistance to a low-resistance state, conducting surge currents to ground and protecting electrical equipment from overvoltage damage.

Since the varistor effect in doped ZnO ceramics was discovered in the 1960s, numerous studies have been conducted to enhance the electrical properties of this material. Especially, Matsuoka's research demonstrated that the ZnO varistors doped with Bi_2O_3, Sb_2O_3, CoO, MnO and Cr_2O_3 additives exhibits a very high non-linear coefficient. Based on that, other additives such as NiO, Al_2O_3, Ga_2O_3, SiO_2 and CaO have been continuously researched to raise the breakdown voltage, the non-linear coefficient, reduce leakage current, and improve the operating stability of the material. Studies have also indicated that the electrical properties of ZnO varistors primarily depend on the grain boundary structure and the Schottky potential barriers formed at grain-to-grain contact regions between ZnO grains.

Nowadays, most commercial varistors are fabricated from micro-sized ZnO powder. However, strong grain growth during the sintering process reduces the grain boundary density, thereby limiting further increases in the breakdown voltage and the non-linear coefficient of the material. In contrast, nano-sized ZnO possesses a large specific surface area, high uniformity, and better sinterability. Using nano - ZnO enhances diffusion and reaction with additives, creating a more uniform microstructure, reducing defects, and improving the quality of the grain boundary region. Concurrently, the small grain size after sintering increases the grain boundary density, contributing to a higher breakdown voltage and non-linear coefficient of the material.

Besides utilizing nano-ZnO, rare-earth elements are considered a potential group of additives to improve the electrical pecifications of ZnO varistors. Rare-earth elements can create charge trap levels at the grain boundaries, increasing the potential barrier height and enhancing the non-linearity of the material. Among them, Pr_6O_{11} is evaluated as a highly promising additive due to its ability to exist in different valence states (Pr^{3+}/Pr^{4+}), which helps modulate the electronic state density at the grain boundaries. The presence of Pr_6O_{11} assists in increasing the Schottky potential barrier height, reducing leakage current, and enhancing the non-linear coefficient of ZnO varistors.

Furthermore, CaO is also an important additive for the ZnO varistors. The addition of CaO helps regulate the grain growth process, increases the density of the material, and raises the potential barrier height at the grain boundaries, consequently, it helps enhancing the non-linear coefficient and reducing leakage current. However, the effect of CaO as well as the interaction between CaO and Pr_6O_{11} in nano-ZnO varistors has not yet been fully researched.

Therefore, this doctoral thesis, entitled **"Study on fabrication and characterization of high-breakdown-voltage varistor based on nano-ZnO and oxide additives"** investigates the effects of Pr_6O_{11} and CaO on the microstructure, electrical characteristics, breakdown voltage, and surge current withstand capability of nano-ZnO varistors, providing a basis for the development of high-performance surge arrester materials

1. Research goals

- To study the utilization of nano-sized ZnO material as the matrix phase for varistors, adjusting the sintering process to control the microstructure and increase the breakdown voltage or breakdown voltage field.
- To research the effects of CaO and Pr_6O_{11} contents and sintering process on the structure and electrical properties of ZnO varistors.
- To investigate the relationship between CaO and Pr_6O_{11} additive compositions and the fabrication process on the microstructure and non-linear characteristics of the varistors, including breakdown voltage (breakdown voltage field), non-linear coefficient, and leakage current, thereby optimizing both the composition and fabrication conditions.

2. Research Contents

- ZnO varistors with 5 basic oxide additives (Bi_2O_3, Sb_2O_3, MnO, Co_3O_4 and Cr_2O_3) are fabricated under different conditions, such as compression pressures and sintering temperatures, and these parameters are optimized through structural morphological characteristics, X-ray diffraction patterns, and electrical properties.
- Nano-ZnO varistors with 5 basic oxide additives blended with CaO are fabricated under different sintering temperatures and sintering times. Their structural morphological characteristics, diffraction patterns, and electrical properties are investigated to optimize the technological conditions as well as the CaO content.
- Nano-ZnO varistors with 5 basic oxide additives (Bi_2O_3, Sb_2O_3, MnO, Co_3O_4 and Cr_2O_3) are mixed with the optimized content of CaO and varying contents of Pr_6O_{11}, and are fabricated under different sintering temperatures and times. Their structural morphological characteristics, diffraction

patterns, and electrical properties are also examined to optimize the technological conditions and the Pr_6O_{11} content.

- The influence of the silver-coated electrode area on the electrical properties of the varistors, physical-mechanical properties (density, shrinkage, and hardness), are investigated to evaluate the appropriate I-V characteristic measurement method and the mechanical strength of the material.

3. Scientific significance

- The thesis contributes to explaining the effect of Pr_6O_{11} content when combined with CaO and sintering technological conditions on the microstructure, phase composition, and electrical properties of the Bi-doped ZnO varistors containing basic oxide additives. Through the investigation of morphological characteristics, X-ray diffraction patterns, and electrical properties, the thesis identifies the optimum Pr_6O_{11} content and sintering process to enhance the non-linear coefficient, increase the break down electric field (voltage), and reduce the leakage current of the varistor.

- The results of the thesis initially demonstrate the prospects of the fabrication of CaO containing varistors with high break down electric fields and low leakage currents at a commercial scale for application in manufacturing surge arresters for high-voltage power systems.

4. New contributions of the thesis

- Scientifically, the necessity of applying the electrode area correction method according to ASTM D257 to obtain the most accurate electrical specifications of the varistors is proven. Specifically, the effective electrode diameter (D_e) should be increased by a fringing effect equivalent to 0.883xh when the gap between the two electrode edges g and the varistor thickness h satisfy the condition $g/h > 10$.

- The thesis contributes to clarifying the positive efficiency of using nano-ZnO to replace micro-ZnO, as demonstrated by the ability to significantly increase the break down electric field, increase the non-linear coefficient α, and remarkably reduce the leakage current of ZnO varistors containing Bi_2O_3, Sb_2O_3, MnO, Co_3O_4 và Cr_2O_3 additives (the ZnO-Bi varistors).

- The thesis clarified the effect of CaO additive content through the use of a nano $CaCO_3$ precursor, as well as fabrication conditions such as sintering temperature and sintering time, on the structure and properties of the varistors. At appropriate CaO content, sintering time and temperature, CaO can significantly increase the non-linear coefficient α, the break down electric field, and reducing the leakage current of the ZnO-Bi varistors.

- The thesis contributes to clarifying the effect of Pr_6O_{11} content when combined with CaO and sintering process on the microstructure, phase composition, and electrical properties of the Bi-doped ZnO varistors containing basic oxide additives. Through the investigation of morphological characteristics, X-ray diffraction patterns, and electrical properties, the thesis determines the optimal Pr_6O_{11} content and sintering regime to enhance the non-linear coefficient, raise the break down electric field, and reduce the leakage current of the varistor.

- The results of the thesis initially demonstrate the potential of fabricating high-performance varistors using nano-ZnO applied in manufacturing surge arresters for high-voltage power grids.

5. Structure of the thesis:

The thesis consists of 140 pages, including: Introduction; Overview of ZnO varistor materials and doping with Pr_6O_{11} and CaO Rare-Earth additives; Research methods; Experimental results and Discussion; Conclusions.

CHAPTER 1. OVERVIEW

1.1. Introduction to ZnO-based varistors

Varistors are non-linear resistors widely utilized in overvoltage protection devices due to their capability to ignificantly vary their resistance as a function of the applied voltage. Among them, zinc oxide (ZnO)-based varistors (metal oxide varistors – MOVs) are the most common type owing to their high non-linear characteristics, fast response time, and high reliability. The material comprises ZnO grains interconnected via grain boundary phases containing additives such as Bi_2O_3, Sb_2O_3, Co_3O_4, MnO_2, Cr_2O_3 and rare-earth oxides. ZnO acts as the semiconducting matrix phase, whereas the additives participate in forming the grain boundary structure and the Schottky potential barriers, which etermining the electrical properties of the material.

The outstanding characteristic of ZnO varistors is their strong non-linear characteristic (Current-Voltage), which is described by the expression $I = kV^{\alpha}$, where α is the non-linear coefficient. A higher α value signifies more effective protection against overvoltage. The operating mechanism of the varistors is directly related to the electronic potential barriers at the ZnO grain boundaries. At normal operating voltages, these potential barriers prevent the movement of electrons, resulting in a very low leakage current. Upon the occurrence of an overvoltage surge, the potential barrier height drops sharply, the material transition into a highly conductive state and conducts large surge currents to the ground, thereby protecting the electrical equipment.

The electrical properties of a varistor depend closely on its material microstructure, particularly the ZnO grain size, grain boundary density, and the distribution of secondary phases. The additives such as Bi_2O_3, Sb_2O_3, Co_3O_4, MnO_2 and Cr_2O_3 play a role in forming liquid-phase, controlling grain growth, and creating of electron trap levels at the grain boundaries, while rare-earth oxides improve the potential barrier height and enhance the non-linearity. The key parameters of a varistor include the break down voltage, non-linear coefficient, leakage current, and surge withstand capability.

1.2. Basic parameters of ZnO varistors and surge arresters

1.2.1. Voltage-Ampere characteristics and non-linear coefficient

The current-voltage characteristic of the material consists of three distinct regions: Region I (pre-breakdown region), characterized by high resistance and low leakage current; Region II (non-linear or breakdown region), where the current increases rapidly with voltage and determines the protective capability of the varistors; and Region III (post-breakdown region), which appears at high current densities when the non-linear characteristic gradually decreases and shifts toward near-linear behavior.

1.2.2. Reference voltage (U_{nmA}), threshold voltage, and breakdown voltage

The reference voltage of a ZnO varistor (U_{nmA}) is the voltage measured at a specified current density. Typically, the reference voltage U_{1mA} corresponds to a current density of 1 mA/cm^2 and is used to evaluate the electrical parameters of the material. The breakdown voltage is the voltage value at which the material transitions from an insulating state to a highly conductive state.

1.2.3. Continuous operating voltage and residual voltage

The continuous operating voltage is the maximum phase-to-ground voltage that can be continuously applied to the varistors or surge arrester over the long term without causing degradation of the device's performance. According to IEC standards, this value is usually equal to approximately 80% of the reference voltage U_{1mA}. The residual voltage is the maximum voltage generated across the terminals of the varistors/surge arrester under the impact of high-intensity standard current surges (typically with an t 8/20μs waveform as 1.0, 2.5, 5.0, 10, 15, and 20 kA).

1.2.4. Leakage current (I_L)

The leakage current (I_L) is the extremely small current that flows through the ZnO varistors when the applied voltage is lower than the threshold voltage, typically determined at approximately 0.5–0.8 times the reference voltage U_{1mA}. The value of the leakage current depends strongly on the material microstructure, particularly the height and uniformity of the potential barriers.

1.3. Worldwide research on ZnO varistors for surge arresters

Worldwide research on ZnO varistors focuses on several main directions: (i) Optimizing additive compositions and fabrication technologies to enhance the non-linear coefficient, reduce leakage current, and increase breakdown voltage; (ii) Developing varistors from nano-sized ZnO using chemical synthesis techniques such as sol-gel, co-precipitation, microemulsion, spray pyrolysis, and combustion synthesis to control grain size and improve electrical properties; (iii) Doping rare-earth oxides (REOs) into the ZnO–Bi_2O_3 varistors to form pyrochlore phases, stabilize the grain boundary microstructure, and enhance non-linear characteristics; (iv) Researching the ZnO - Pr_6O_{11} varistors combined with other metal and rare-earth additives to overcome the inherent limitations of the Pr_6O_{11} varistors, thereby improving stability, breakdown voltage, and energy absorption capability.

1.4. Domestic research on ZnO varistors

In Vietnam, research primarily focuses on the fabrication and application of ZnO varistors for surge protection devices, the optimization of additive compositions, and the development of powder synthesis technologies via spray pyrolysis and co-precipitation methods. Concurrently, domestic studies the effects of rare-earth elements and sintering conditions on the microstructure and electrical properties of the varistors.

CHAPTER 2. RESEARCH METHODS

2.1. Materials and chemicals

Micro-ZnO (mZnO, 99.0%) powder with an average particle size of approximately 1 µm. Nano-ZnO (nZnO, 99.0%) powder with a particle size ranging from 20 to 100 nm (average size of 50nm). Bismuth oxide (Bi_2O_3, 99.0%), antimony oxide (Sb_2O_3, 99.5%), chromium oxide (Cr_2O_3, 99.0%), ethanol (99.8%), manganese dioxide (MnO_2, 85%), cobalt oxide (Co_3O_4, 98%), praseodymium oxide (Pr_6O_{11}, 99.9%, 100 mesh), nano $CaCO_3$ (99.5%, 50 nm).

2.2. Varistors fabrication

2.2.1. Fabrication of micro-ZnO varistors for electrode area analysis

The ZnO varistors were fabricated with a fixed composition of ZnO : Sb_2O_3 : Bi_2O_3: MnO_2 : Co_3O_4: Cr_2O_3 = 96.5 : 1.25 : 1.25 : 0.5 : 0.5 : 0.5 mol%, through ball milling, drying, mixing with 2% PVA, and disc pressing. Subsequently, the samples were pre-fired at 600 ^oC for 1 h and sintered at 1000 ^oC for 2 h.

2.2.2. Fabrication of varistors using micro-ZnO and nano - ZnO for investigation of compaction pressure, sintering temperature, and sintering time.

ZnO varistors were fabricated with the composition ZnO (nano or micro) : Bi_2O_3 : Sb_2O_3: MnO_2 : Co_3O_4: Cr_2O_3 = 96.5 : 1.25 : 1.25 : 0.5 : 0.5 : 0.5 mol%, through ball milling steps with 2% PVA. Afterwards, the samples were dried, and were investigated the conditions such as: the pressing force, sintering temperature, and sintering time.

Nano-ZnO and Micro-ZnO varistors were investigated for pellet pressing pressure from 50, 75, 100 and 125 to 150 Mpa.

Nano-ZnO varistors were investigated at sintering temperature of 1000 ^oC, 1050 ^oC, 1100 ^oC, 1150 ^oC and 1200 ^oC. The elletizing pressure was kept fixed at 100 MPa, and the sintering time was fixed for 2 hours.

After selecting the optimal sintering temperature of 1050 ^oC, the sintering time were investigated at 1h, 2h, 3h, and 4h.

2.2.3. Synthesis of ZnO nanoplates by hydrothermal method and fabrication of varistors from ZnO nanoplates

Plate-shaped nano-ZnO was synthesized by the hydrothermal method from $ZnSO_4.7H_2O$, using urea to adjust pH and conducting the reaction in an autoclave at 220 ^oC for 24 hours. The product was then washed clean, dried, and calcined at 600 ^oC to complete the crystal structure of plate-shaped nano-ZnO.

The investigated varistors had the composition as follows: ZnO (Nanoplate) : Bi_2O_3 : Sb_2O_3: MnO_2 : Co_3O_4: Cr_2O_3 : $CaCO_3$ = X : 1.5 : 1.25 : 0.8 : 0.4 : 0.25: Y mol%, through ball milling steps with 2% PVA. Afterwards, the samples were dried, pressed into pellets, sintered, and coated with silver electrodes to test the specifications.

2.2.4. Fabrication of CaO-doped varistors with different contents

The varistors investigated for content had the composition as follows: ZnO (nano) : Bi_2O_3 : Sb_2O_3: MnO_2 : Co_3O_4: Cr_2O_3 : $CaCO_3$ = X : 1.5 : 1.25 : 0.8 : 0.4 : 0.25: Y mol%, through ball milling steps with 2% PVA. The nano-ZnO content was X = 95.80; 95.30; 94.80; 94.30; 93.80 corresponding to the CaO content Y = 0; 0.5; 1; 1.5; 2. The material mixture doped with CaO according to the above investigated contents was then pressed into disc pellets under 100 MPa pressure. The samples were pre-fired at 600 ^oC for 1 h, sintered at 1000 ^oC for 2 h, and cooled. The varistor samples were ground, polished, coated with silver electrodes, and tested for properties.

2.2.5. Fabrication of varistor samples co-doped with CaO and Pr_6O_{11}

Nano-ZnO varistors with the composition of 5 basic additive oxides and 1% CaO doped with Pr_6O_{11} were as follows: ZnO (nano) : Bi_2O_3 : Sb_2O_3: MnO_2 : Co_3O_4: Cr_2O_3 : $CaCO_3$: Pr_6O_{11} = X : 1.5 : 1.25 : 0.8 : 0.4 : 0.25: 1: Y mol%, through ball milling steps with 2% PVA. The nano-ZnO content was X = 94.80; 94.68; 94.55; 94.30 corresponding to the Pr_6O_{11} content Y = 0; 0.125; 0.25 and 0.5. The material mixture doped with Pr_6O_{11} according to the above investigated contents was then pressed into disc pellets under 100 MPa pressure. The samples were pre-fired at 600 ^oC for 1 h, sintered at 1050 ^oC for 3 h, and cooled. The varistors were ground, polished, coated with silver electrodes, and tested for properties.

2.2.6. Fabrication of large-sized high-surge-current varistors for testing and surge arrester assembly

The varistors using nano-ZnO and 5 basic additive oxides doped with 1% CaO had the composition as follows: ZnO (nano) : Bi_2O_3 : Sb_2O_3: MnO_2 : Co_3O_4: Cr_2O_3 : $CaCO_3$= 94.8 : 1.5 : 1.25 : 0.8 : 0.4 : 0.25: 1 and were ball milled with 2% PVA. The material mixture was then pressed into disc pellets under 100 MPa pressure. The samples were pre-fired at 600 °C for 1 h, sintered at 1050°C for 3 h, and cooled. The varistors were ground, polished, arc-sprayed with metal oxide aluminum electrodes, and tested for properties.

2.3. Research methods

2.3.1. Microscopic method: Using the JSM-6510LV scanning electron microscope (SEM).

2.3.2. XRD method: Using the Bruker D8 Advance (Germany).

2.3.3. Determination of shrinkage, bulk density, and hardness: The density use a 6-digit analytical balance (AS220.R2PLUS, Radwag, Poland). The hardness was measured using Vickers hardness tester (NEXUS 7700 - Innovatest, Netherlands).

2.3.4. Method for determining Volt-Ampere (I-V) characteristics: Using the GW INSTEX - GPT9802A electrical safety testing equipment.

2.3.5. Method for measuring complex impedance and dielectric constant: Using the Precision LCR meter Agilent E4980A (Keysight, USA) and the multichannel electrochemical workstation Biologic VSP300

2.3.6. Error evaluation of electrical parameters: The accuracy of the electrical parameters in the study was evaluated based on the accuracy of the measuring instruments combined with relative errors.

CHAPTER 3. RESULTS AND DISCUSSION

3.1. Effect of electrode area correction on the electrical properties of varistors

Three methods for calculating the effective electrode diameter D of the varistors (Arithmetic mean method of two electrode diameters – Method 1, Geometric mean method – Method 2, and Geometric mean method considering the electric field fringe effect – Method 3) (Table 3.1).

Method 1	Method 2	Method 3
$D = \frac{D_1 + D_2}{2}$	$D = \sqrt{D_1 D_2}$	$D_{1e} = D_1 + 0.883\times h$ $D_{2e} = D_2 + 0.883\times h$; $D = \sqrt{D_{1e} D_{2e}}$

Table 3.1. Three methods for determining the electrode

Studies have shown that the method used to determine the electrode area significantly affects the accuracy of the obtained electrical parameters.

3.1.1. Reference voltage (U_{1mA} and U_{10mA}) of the varistors

All three methods showed good linear relationships between voltage and sample thickness (Figure 3.1). However, method 3 yielded the best result with the highest correlation coefficient R^2 = 0.9997 and the lowest dispersion.

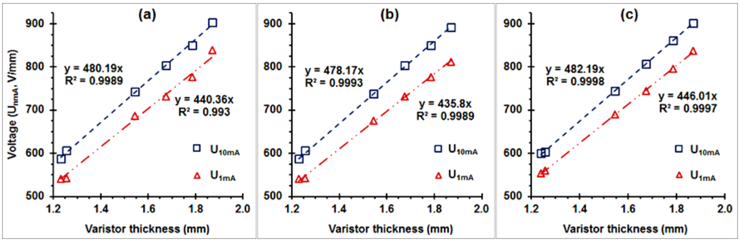

Figure 3.1. Variation of U_{1mA} và U_{10mA} as a function of varistor sample thickness when the electrode diameter D is determined by three different methods.

3.1.2. Nonlinear coefficient of the varistors

Method 3 yielded optimal results with α = 29.5 ± 1.0 which is higher and more stable than those obtained from Methods 1 and 2 (Table 3.2). Correcting for the electric field fringe effect helped to accurately determine the current density and the nonlinear characteristics of the material.

Table 3.2. Values of the nonlinear coefficient α determined by different methods

Samples	Method 1		Method 2		Method 3	
	S (cm^2)	α	S (cm^2)	α	S (cm^2)	α
D4.4	0.127	20.8	0.127	20.8	0.205	28.0
D8.8	0.575	24.9	0.575	24.9	0.807	29.0
S10.10	0.880	28.3	0.880	28.3	1.074	30.9
D10.10	0.972	25.0	0.972	25.0	1.248	28.5
D6.16	0.965	29.2	0.771	26.1	0.943	30.1
D3.16	0.729	31.2	0.403	24.6	0.611	30.6
Average	-	26.6 ± 3.0	-	24.9 ± 1.5	-	29.5 ± 1.0

3.1.3. Volt-Ampere (I-V) characteristics of the varistors

The (J-E) and Log(ρ) - E curves show that when Method 3 is applied, the curves of samples with different electrode sizes almost perfectly overlap,

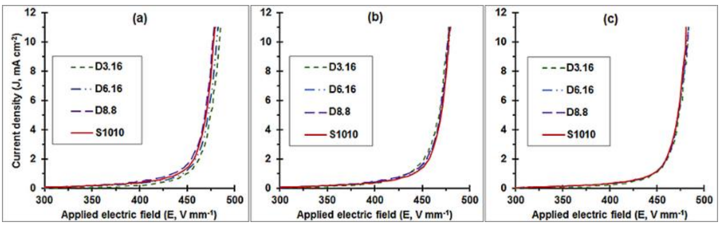

Figure 3.2. J – E curves of the ZnO varistors using three different methods for determining the electrode area.

proving that the effective electrode area is determined most consistently with reality. Conversely, Methods 1 and 2 still show significant deviations, especially for samples with asymmetric electrodes (Figure 3.2).

3.1.4. Electrical resistivity of the varistors The investigation of the Log(ρ) - E characteristics shows that the determination of the electrode area significantly affects the electrical resistivity values of the ZnO varistors. Method 3 yields curves that almost perfectly overlap in the breakdown region, accurately reflecting the bulk conduction behavior when the Schottky barriers at the grain boundaries are broken. This confirms the high reliability and necessity of applying the electrode area correction.

3.2. Effect of compaction pressure on varistors

3.2.1. Structural morphology of ZnO varistors (micro and nano)

When the compaction pressure increased from 50 to 150MPa, the microstructure of the ZnO varistors becomes denser, porosity decreases, and intergranular bonding is significantly improved. The optimal range of 100 Mpa to 125 Mpa, yields high bulk density and the most uniform microstructure. The nano-ZnO samples exhibit smaller and more uniform grain sizes compared to the micro-ZnO samples: the NanoP sample averages 3.19 ± 0.8 µm (predominantly 2 ± 4 µm) (Figure 3.10), whereas the MicroP sample averages 3.68 ± 1.3 µm (with a wide distribution of 1 - 6 µm) (Figure 3.11). However, when the compaction pressure were increasing to 150 MPa, despite of the increased density, the risk of sample cracking and deformation becomes significantly higher; thus, the optimal compaction pressure is in the range of 75 to 100 MPa.

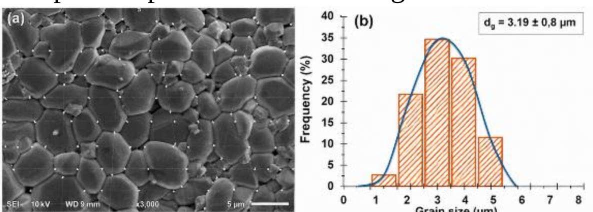

Figure 3.10. (a) Schematic illustration of the linear intercept method for grain counting and (b) grain size distribution of the NanoP50 ZnO varistor.

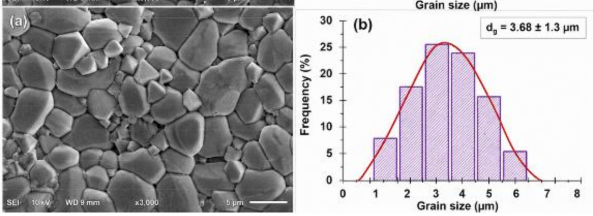

Figure 3.11. (a) Schematic illustration of the linear intercept method for grain size calculation and (b) grain size distribution of the MicroP50 varistor.

Due to its narrow and uniform size distribution, the NanoP sample achieves higher bulk density, reduced post-sintering porosity, and a more stable microstructure.

3.2.2. I-V characteristics and nonlinear coefficient of ZnO varistors

Study indicate that compaction pressure significantly influences the electrical specifications of ZnO varistors. For the NanoP varistors, a compaction pressure of 75 Mpa, yields optimal performance with a nonlinear coefficient α = 54.2, a leakage current density J_L = 1.3 µA/cm^2 and a breakdown electric field E_{1mA} = 800 V/mm (Figure 3.12 and Table 3.3). For the MicroP varistors, the compaction pressure at 75 MPa also demonstrates optimal properties, with α = 53.1, J_L = 1.32 µA/cm^2, and E_{1mA} = 612 V/mm (Figure 3.13 and Table 3.4). When compaction pressure increases, E_{1mA} progressively increases, whereas α tends to decrease. Compared to MicroP, the NanoP samples exhibit a higher breakdown electric field by approximately 25 - 33%, demonstrating the superiority of nano-ZnO materials. Overall, the results showes that the optimal compaction pressure range of 75 – 100 Mpa for both nano ZnO and micro ZnO.

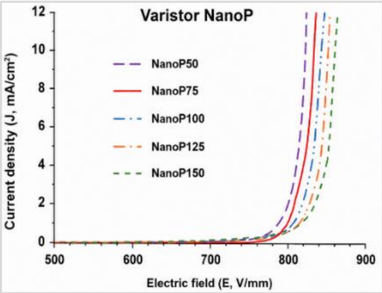

Figure 3.12. Voltage-Ampere (E-J) characteristics of NanoP varistors compacted at various pressures.

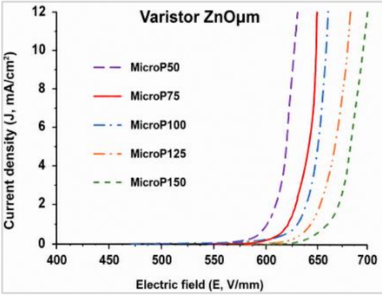

Figure 3.13. Voltage-Ampere (E-J) characteristics of MicroP varistors compacted at various pressures.

Table 3.3. Electrical properties of NanoP varistors.

Sample	**E_{1mA} (V/mm)**	**E_s (V/mm)**	**J_L (µA/cm^2)**	**α**
NanoP50	788 ± 1.5	591 ± 1.2	2.1 ± 0.02	51.6 ± 0.5
NanoP75	800 ± 1.8	600 ± 1.5	1.3 ± 0.01	54.2 ± 0.6
NanoP100	806 ± 1.6	604 ± 1.5	3.8 ± 0.02	53.2 ± 0.6
NanoP125	813 ± 1.8	610 ± 1.6	3.7 ± 0.02	51.3 ± 0.5
NanoP150	816 ± 1.9	612 ± 1.6	4.2 ± 0.02	44.3 ± 0.3

Table 3.4. Electrical properties of MicroP varistors.

Sample	**E_{1mA}(V/mm)**	**E_s (V/mm)**	**J_L (µA/cm^2)**	**α**
MicroP50	592 ± 1.3	444 ± 1.0	2,3 ± 0.02	51.1 ± 0.5
MicroP75	612 ± 1.4	459 ± 1.0	1.3 ± 0.01	53.1 ± 0.6
MicroP100	620 ± 1.5	465 ± 1.1	1.6 ± 0.01	52.8 ± 0.5
MicroP125	634 ± 1.5	475 ± 1.1	2.2 ± 0.02	44.1 ± 0.2
MicroP150	649 ± 1.7	487 ± 1.2	2.9 ± 0.02	41.5 ± 0.2

3.2.3. Dielectric properties of the ZnO nanoP varistors

The dielectric constant ε′ of NanoP decreases sharply with frequency, dropping from (4 - 5)×10^3 to 300 - 400 (NanoP100), while tanδ decreases from 9 - 10 to near zero due to the decrease of space charge polarization. When the compaction pressure increases from 50 to 150 MPa, ε′ increases due to the increase in grain boundary interfaces and charge trapping center. These results show that the dielectric pecifications depend significantly on both frequency and compaction pressure (Figure 3.14).

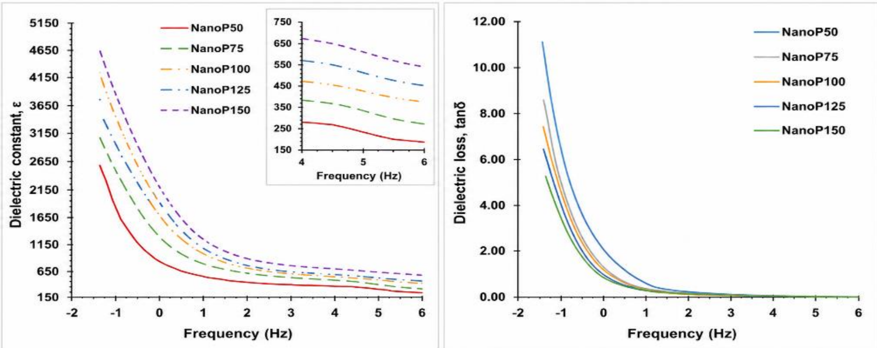

Figure 3.14.(a) Dielectric constant and (b) Dielectric loss of NanoP ZnO varistors.

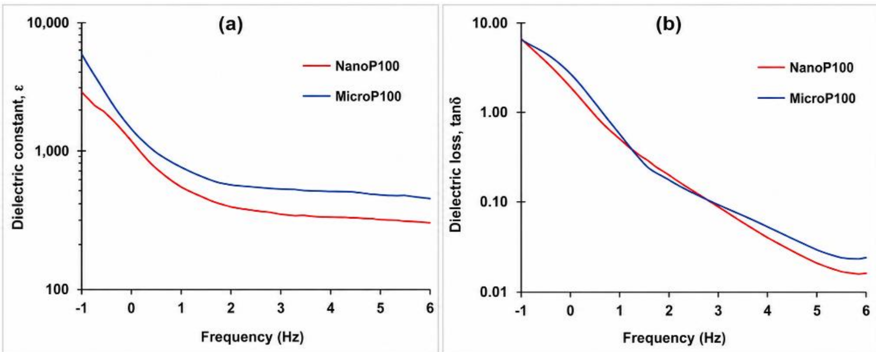

Figure 3.15. (a) Dielectric constant and (b) Dielectric loss of NanoP100 and MicroP100 ZnO varistors.

Figure 3.15 shows that ε′ for both NanoP100 and MicroP100 samples decreases sharply when the frequency increases from 10^{-1} đto 10^6 Hz, with MicroP100 exhibiting higher values in the low-frequency region owing to strong space charge polarization at the grain boundaries. As the frequency increases, ε′ decreases rapidly and then saturates due to the transition from space charge polarization to electronic and ionic polarization. Meanwhile, tanδ drops from approximately 9 - 10 to near zero, reflecting a reduction in conduction loss and slow polarization processes. The difference between the two samples decreases significantly in the high-frequency region.

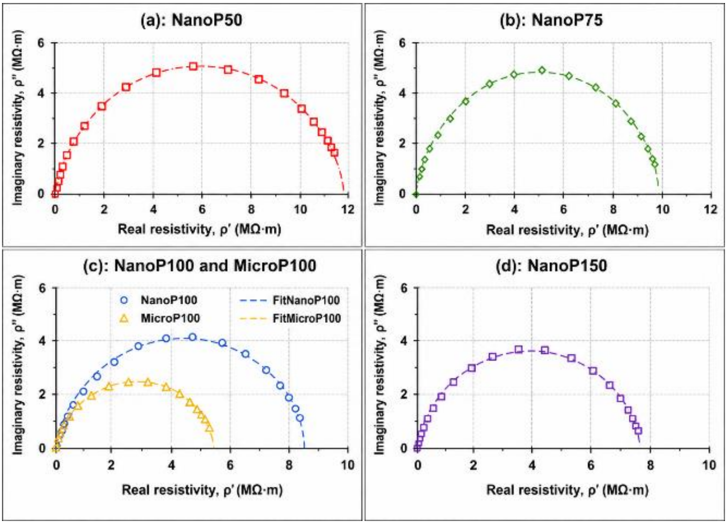

Figure 3.16. Cole–Cole complex resistivity plots of NanoP varistors

The Cole–Cole plots (Figure 3.16) and Table 3.5 demonstrate that the grain boundary resistivity decreases from 11.87 MΩ.m (NanoP50) to 7.49 MΩ.m at higher compaction pressures. The NanoP100 sample achieves optimal dielectric properties and electrical resistance, with ρ'_o = 0.06 Ω.m and ρ'_{gb} = 8.35 MΩ.m, indicating a good balance between polarizability and electrical conductivity of the material.

Table 3.5. Resistance and resistivity of NanoP varistors.

Samples	**R_o (Ω)**	**Grain interior resistivity ρ'_0 (Ω.m)**	**R_{gb} (MΩ)**	**Grain boundary resistivityρ'_{gb} (MΩ.m)**
NanoP50	1.76	0.22	94.13	11.87
NanoP75	1.76	0.19	89.57	9.77
NanoP100	1.15	0.06	102.03	8.35
NanoP150	0.87	0.18	82.36	7.49

Summary of Section 3.2: Compaction pressure significantly influences the microstructure, mechanical strength, and electrical specifications of ZnO varistors by promoting material densification, reducing porosity, and improving homogeneity. At approximately 75 - 100 MPa, the microstructure reaches an optimal state, yielding superior mechanical hardness and high electrical nonlinearity. Conversely, excessive compaction pressure degrades the potential barrier and may cause microdefects. Comparison of the two systems shows that nano-sized ZnO exhibits a more uniform microstructure better electrical properties than micro-sized ZnO.

3.3. Properties of varistors using plate-like ZnO

3.3.1. Structure and properties of plate-like ZnO materials

SEM images show that micro-ZnO possesses a grain size of approximately 1 µm, while ZnO nanoplates synthesized via the hydrothermal method exhibit a thickness of around 15 nm and a length ranging from 100 – 400 nm (Figure 3.17).

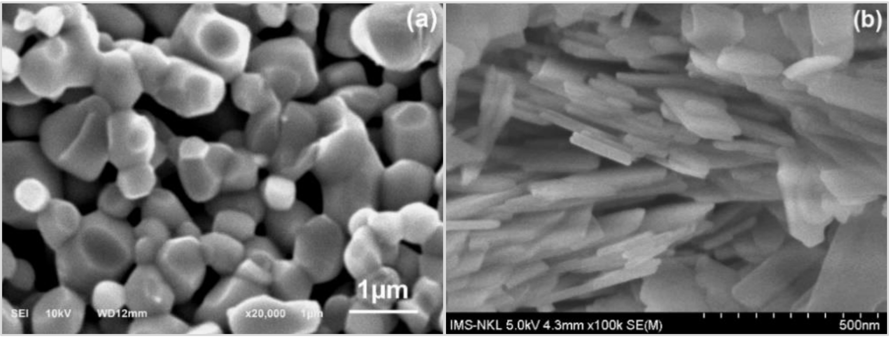

Figure 3.17. SEM images of micro-ZnO (a) and synthesized ZnO nanoplates (b)

The FTIR spectra (Figure 3.18a) display the characteristic Zn-O absorption band below 600 cm^{-1}, along with the adsorption peaks of -OH groups (~3400 cm^{-1}) and adsorbed water (~1630 cm^{-1}) in the nanoplate sample. The XRD results indicate that both sample exhibit the wurtzite ZnO structure with crystal planes (100), (002), (101), (102), (110), (103), and (112), and no other additives are detected. The diffraction peaks of the ZnO nanoplates are broader and show a preferred orientation along the (002) plane, reflecting small crystallite size and a nanoplate structure (Figure 3.18b).

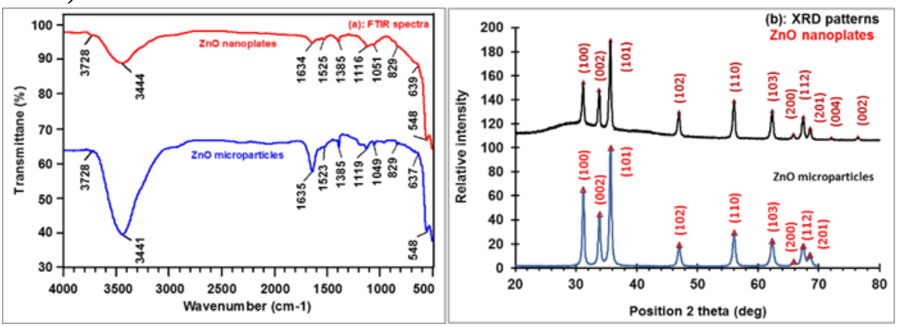

Figure 3.18. (a) FTIR spectra and (b) XRD patterns of micro-ZnO and ZnO nanoplate varistors.

3.3.2. Morphological and structural of varistors fabricated from micro-ZnO and nano-ZnO

XRD results show that all samples exhibit the hexagonal wurtzite ZnO structure corresponding to the (100), (002), (101), (102), (110), (103), and (112) planes, and the presence of a $Zn_{1,82}Cr_{0,78}Sb_{0,41}O_4$ spinel phase (Figure 3.19). The grain size of the nano-based varistors increases from 1.7 ± 0.2 µm (NanoZ1000) to 3.5 ± 0.3 µm (NanoZ1100) and 5.5 ± 0.6 µm (NanoZ1200), whereas the MicroZ1100 varistor reaches 4.7 ± 0.6 µm (Table 3.6). As the sintering temperature increases, grain growth occurs in all samples due to strong diffusion; however, the micro-based varistors grow faster.

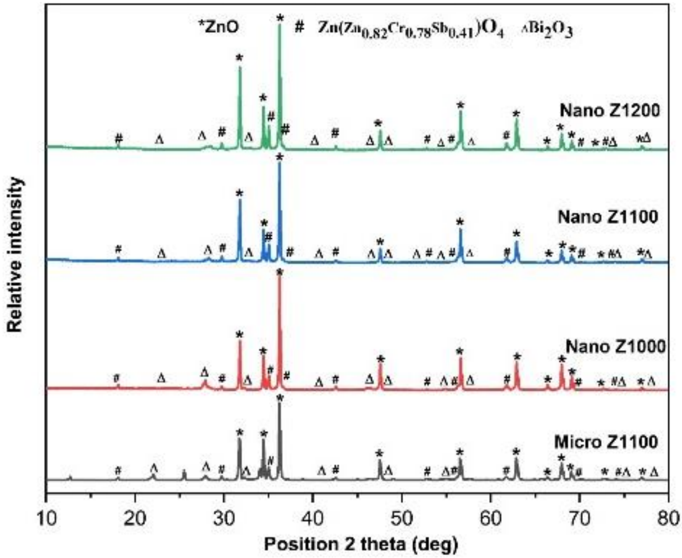

Figure 3.19. XRD patterns of nano and micro-ZnO varistos sintered at various temperatures.

Table 3.6. Grain sizes of nano-ZnO varistors

Sample	Sintering Temperature (°C)	Surface Grain Size (µm)	Cross-Sectional Grain Size (µm)
NanoZ1000	1000	1.7 ± 0.2	1.8 ± 0.3
NanoZ1100	1100	3.5 ± 0.3	3.8 ± 0.3
NanoZ1200	1200	5.5 ± 0.6	6.8 ± 1.0
MicroZ1100	1100	4.7 ± 0.6	4.8 ± 0.9

3.3.3. Current - Voltage characteristics and electrical properties of ZnO varistors

All ZnO varistors exhibit typical nonlinear behavior, characterized by a sharp decrease in resistivity upon reaching the breakdown electric field. The sintering temperature significantly influences the electrical properties of the ZnO varistors. When the sintering temperature increases from 1000 °C to 1200 °C (Figure 3.22), the breakdown electric field of the nano ZnO varistors decreases from 1336 to 286 V/mm, due to grain growth reducing the grain boundary density (Table 3.7). Compared to the micro-ZnO varistors, the nano-ZnO varistors exhibits higher resistivity in the low-field region and displays a higher nonlinearity when transitioning into the breakdown region (Figure 3.23).

Table 3.7. Summary of electrical properties of the investigated varistor samples.

Sample	U_{gb} (V)	E_{1mA} (V/mm)	α	J_L (μA/cm^2)
NanoZ1000	2.41	1336 ± 2.4	34.3 ± 0.5	11.9 ± 0.1
NanoZ1100	2.62	689 ± 1.2	48.5 ± 0.8	9.7 ± 0.1
NanoZ1200	1.94	286 ± 0.8	24.6 ± 0.4	27.6 ± 0.2
MicroZ1100	2.07	432 ± 1.0	35.8 ± 0.5	23.4 ± 0.2

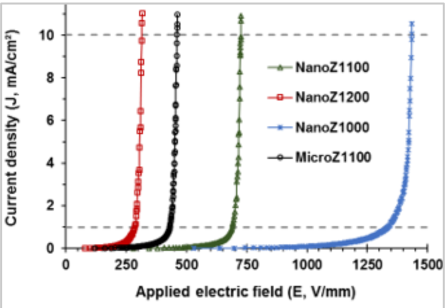

Figure 3.22. E – J curves of nano-ZnO and micro-ZnO varistors at various sintering temperatures.

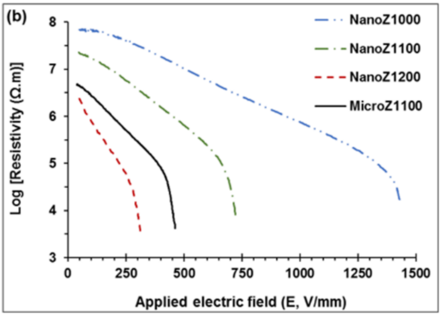

Figure 3.23. Resistivity curves of micro and nano-ZnO varistors.

3.3.4. Impedance and AC resistivity specifications of ZnO varistors

When the sintering temperature increases from 1000 °C to 1200 °C, ρ_{gb} of the nano-ZnO varistors decreases sharply from 76.90 to 2.34 MΩ.m (Table 3.8), which is attributed to ZnO grain growth.

Table 3.8. Impedance spectroscopy properties of micro-ZnO varistors.

Sample	R_o (Ω)	ρ_o (Ω.m)	ρ at 2MHz (Ω.m)	ρ_{gb} (MΩ.m)	R_{gb} (Ω)
NanoZ1000	1.97	0.083	11.51	76.90	1829
NanoZ 1100	1.29	0.072	5.03	17.45	312.7
NanoZ 1200	0.81	0.038	1.42	2.34	50.3
MicroZ1100	1.08	0.049	2.64	4.55	100.1

At a frequency of 2 MHz, the AC resistivity of NanoZ1100 reaches 5.03 Ω.m, nearly twice as high as that of MicroZ1100 (2.64 Ω.m). These results indicate that the nano-ZnO varistors exhibits current-blocking capabilities, grain boundary polarization, and form a Schottky potential barrier more effective than the micro-ZnO varistors.

Summary of Section 3.3: Research results show that compacting pressure, ZnO particle size, and sintering temperature significantly influence the microstructure and electrical properties of ZnO varistors. Utilizing hydrothermally synthesized ZnO nanoplates yields a more uniform microstructure and higher grain boundary density, while exhibiting a higher breakdown electric field, a higher nonlinearity coefficient, and lower leakage current compared to the micro-ZnO varistors. The optimal fabrication conditions were identified as a compacting pressure of approximately 100 MPa and a sintering temperature of around 1100 °C, this process suitable for fabricating high-voltage, and high-performance surge-protection ZnO varistors.

3.4. Influence of sintering temperature and time on the crystalline nano-ZnO varistors

3.4.1. Morphological and Structural

When the sintering temperature increases from 1000 °C to 1200 °C, the ZnO grain size increases from 1.53 to 4.59 µm, making a denser microstructure. XRD results indicates that all samples maintain the hexagonal wurtzite ZnO phase, with crystallinity increasing markedly with temperature. However, secondary spinel phases begin to appear at 1200 °C, suggesting that excessively high temperatures can affect the varistor performance.

3.4.2. Current–Voltage characteristics

The current–voltage (I-V) characteristics results show that the sample sintered at 1050°C for 3h (T1050C.3h) exhibits optimal electrical properties, achieving a nonlinearity coefficient $\alpha = 55.02$, breakdown electric field $E_{1mA} = 832$ V/mm and leakage current density $J_L = 1.78$ µA/cm^2(Table 3.9).

Table 3.9. DC electrical properties of ZnO varistors fabricated under various sintering temperatures and times.

Sample	E_{1mA} (V/mm)	α	E_s (V/mm)	E_c (V/mm)	J_L (µA/cm^2)
T1000C	1294 ± 2.4	25.48 ± 0.3	971 ± 1.8	647 ± 1.1	17.47 ± 0.3
T1050C	986 ± 1.8	52.54 ± 0.6	739 ± 1.2	493 ± 1.0	1.56 ± 0.05
T1100C	733 ± 1.2	41.56 ± 0.5	549 ± 1.0	366 ± 1.1	6.93 ± 0.1
T1150C	420 ± 1.0	46.29 ± 0.5	315 ± 0.8	210 ± 0.2	30.20 ± 0.8
T1200C	299 ± 0.6	12.51 ± 0.1	224 ± 0.2	149 ± 0.1	72.47 ± 1.2
T1050C.1h	1085 ± 2.1	37.77 ± 0.4	814 ± 0.5	542 ± 1.0	10.80 ± 0.2
T1050C.2h	986 ± 1.8	52.54 ± 0.6	739 ± 1.3	493 ± 1.0	1.56 ± 0.05
T1050C.3h	832 ± 1.5	55.02 ± 0.7	624 ± 1.1	416 ± 0.9	1.78 ± 0.05
T1050C.4h	779 ± 1.4	55.97 ± 0.8	584 ± 1.0	389 ± 0.8	3.30 ± 0.08

Compared to other processing conditions, this sample demonstrates a good balance of high breakdown field, low leakage current, and strong nonlinearity.

3.4.3. Dielectric Properties

Impedance spectroscopy results indicate that the grain boundary resistivity decreases sharply with increasing sintering temperature, dropping from approximately 93 MΩ.m (T1000C) down to 2.8 MΩ.m (T1200C), which reflects a degradation of the potential barrier height at the grain boundaries. Concurrently, the dielectric constant ε′ increases with sintering temperature; specifically, the T1200C sample reaches approximately 10^4 at 10^{-1} Hz, significantly higher than that of the T1000C sample (≈10^3). The dielectric loss tanδ also increases with temperature, reaching around 30 for T1200C and approximately 8 for T1000C at low frequencies (Figure 3.29).

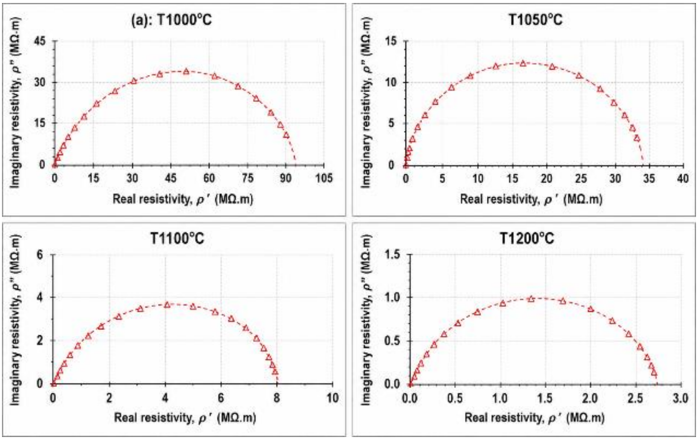

Figure 3.29. Impedance spectra of nano-ZnO varistors sintered at various temperatures: 1000 °C (a), 1050 °C (b), 1100 °C (c), 1200°C (d).

Summary of Section 3.4: The optimal sintering conditions for the ZnO varistors were determined to be 1050 °C for 3 h, yielding a uniform microstructure, high relative density, and stable grain boundaries. Under these conditions, the material achieves best electrical performance, characterized by a high nonlinearity coefficient α ≈ 55, low leakage current density (~1.78 µA/cm^2) and effective surge protection capabilities. These results demonstrate an optimal balance between densification, grain growth, and grain boundary potential barrier formation, suitable for the fabrication of high-quality ZnO varistors.

3.5. Structure and properties of CaO-doped nano-ZnO varistors

3.5.1. Effect of CaO content on the structure and properties of the ZnO varistors

The CaO content has a significant influence on the microstructure and electrical properties of the ZnO varistors. When the CaO content increases from 0 to 1% mol, the nonlinearity coefficient increases from 51.7 to 59.7, while the leakage current density decreases from 5.61 down to 2.15 μA/cm^2 and the grain boundary resistivity rises from approximately 44.65 to 48.86 MΩ.m. However, when the CaO content continues to increase to 1.5 -2% mol, α decreases to 50.6 - 52.3, and the leakage current increases again (Table 3.11 and Figure 3.33).

These results indicate that 1% mol CaO represents the optimal content, offering the best balance between a uniform microstructure and superior electrical performance in ZnO varistors

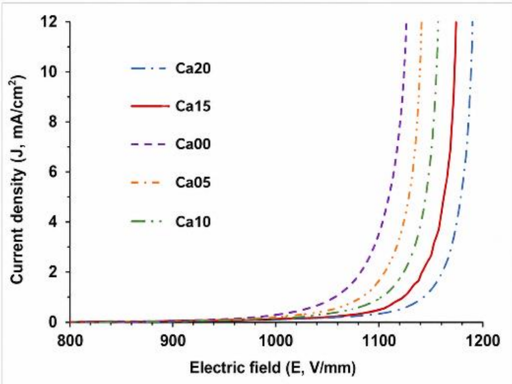

Figure 3.33 (a). Voltage-Ampere (E-J) characteristics of varistors with different CaO molar contents

Table 3.11. DC electrical properties and complex impedance specifications of CaO-doped varistors sintered at different temperatures.

Sample	E_{1mA} (V/mm)	α	E_s (V/mm)	J_L (μA/cm^2)	ρ'_{gb} (MΩ.m)	R_o (Ω)
Ca00	1211 ± 2.1	51.7 ± 0.6	807 ± 0.5	5.61 ± 0.03	44.65	0.254
Ca05	1095 ± 1.8	54.2 ± 0.7	821 ± 0.5	1.61 ± 0.01	46.75	0.224
Ca10	1112 ± 2.0	59.7 ± 0.8	834 ± 0.5	2.15 ± 0.02	48.86	0.226
Ca15	1127 ± 2.0	52.3 ± 0.6	846 ± 0.6	4.68 ± 0.03	50.65	0.231
Ca20	1142 ± 2.0	50.6 ± 0.5	857 ± 0.6	5.35 ± 0.03	52.25	0.235

3.5.2. Effect of sintering temperature

The electrical properties of the ZnO - CaO varistors are strongly dependent on the sintering temperature. At 1000 ^oC, the material exhibits a high breakdown electric E_{1mA} = 1319,5 V/mm but a low nonlinearity coefficient (31.39) and high leakage current density (15.70 μA/cm^2), indicating unactivated grain boundaries. At 1050 ^oC, optimal electrical performance is achieved, with α reaching 54.23, J_L decreasing to 1.61 μA/cm^{2}and the grain boundary resistivity measuring approximately 46.75 MΩ.m, reflecting the formation of well-developed grain boundary potential barriers. When increasing the temperature to 1100 – 1200 ^oC, α decreases to 45.50 - 34.30 and J_L increases significantly, which is attributed to excessive grain growth that degrades the grain boundary region. Consequently, 1050 °C is identified as the optimal sintering temperature for the varistor effect.

3.5.3. Effect of sintering time

Sintered at 1050 °C for 3h, the ZnO–CaO varistor achieves superior electrical specifications with a high nonlinearity coefficient ($\alpha \approx 54.2 - 55{,}8$) and low leakage current density (≈1.61 - 1.68 μA/cm^2), which demonstrates the efficient formation of grain boundary potential barriers. The grain boundary resistivity of 38.9 MΩ.m, ensures an optimal balance between intragranular conduction and grain boundary blocking capability (Table 3.15).

Table 3.15. DC electrical properties and complex impedance parameters of CaO-doped varistors sintered under different sintering times

Sample	E_{1mA} (V/mm)	α	E_s (V/mm)	J_L (μA/cm^2)	ρ'_{gb} (MΩm)	R_o (Ω)
Ca1050t1	1211 ± 2.2	39.7 ± 0.5	909 ± 1.8	19.9 ± 0.3	55.2	0.368
Ca1050t2	1095 ± 2.1	54.2 ± 0.7	821 ± 1.7	1.61 ± 0.05	46.8	0.224
Ca1050t3	819 ± 1.7	55.8 ± 0.7	615 ± 1.2	1.68 ± 0.05	38.9	0.152
Ca1050t4	731 ± 1.5	52.9 ± 0.6	549 ± 1.0	1.17 ± 0.04	20.50	0.096

Summary of Section 3.5: The results show that the optimal doping level of 1% mol CaO significantly enhances the performance of ZnO varistors, with a higher nonlinearity coefficient and a reduced leakage current density due to strengthened grain boundary potential barriers. However, exceeding 1.5% mol CaO reduces microstructural homogeneity and electrical properties. The optimal sintering temperature was determined to be 1050 °C, yielding $\alpha \approx 54.2$ and $J_L = 1.61$ μA/cm^2, whiles higher temperatures degrade performance due to grain growth. The optimal sintering time of 2 - 3 h maintains structural stability, high hardness, and excellent overall electrical specifications.

3.6. Structure and properties of Pr_6O_{11}-doped nano ZnO-Ca varistors

3.6.1. Morphological and structural

Structural analysis results shows that Pr_6O_{11} reduces the ZnO grain size (from ~3.25 down to ~2.82 μm) and significantly suppresses grain growth. However, at higher Pr_6O_{11} concentrations, the microstructure becomes less uniform with the appearance of fine grain clusters and secondary phases at the grain boundaries. FTIR spectra confirm the stability of the ZnO wurtzite lattice, while Pr–O and Bi–O vibrations became more pronounced with increasing Pr. Overall, an optimal Pr_6O_{11} doping concentration of approximately 0.25% mol effectively controls grain size and maintains a homogeneous microstructure.

3.6.2. Shrinkage and hardness

A low level of Pr_6O_{11} improves the microstructure and mechanical properties of the ZnO–Bi–Ca varistors by promoting the sintering process and enhancing material homogeneity. When the doping concentration exceeds the optimal threshold, sintering is suppressed, and the appearance of secondary phases degrades relative density and mechanical strength.

3.6.3. Current–Voltage characteristics

Current-voltage (I-V) characteristics demonstrate that Pr_6O_{11} significantly enhances the nonlinearity of the ZnO-Bi-Ca varistors. Within the optimal concentration range, Pr_6O_{11} promotes the grain boundary potential barrier height and enhances the breakdown electric field. The presence of Pr at the grain boundaries creates deep-level traps, thereby enhancing stability, reducingleakage current density, while also increasing grain boundary resistivity. When the optimal content is exceeded, nonlinearity decreases due to the formation of secondary phases and reduced microstructural uniformity (Table 3.17).

Table 3.17. DC electrical properties and complex impedance parameters of ZnO-Bi-Ca varistors with different Pr_6O_{11} contents (sintered at 1050 °C for 3h).

Sample	E_{1mA} (V/mm)	α	E_s (V/mm)	J_L (μA/cm^2)	ρ'_{gb} (MΩ.m)	R_o (Ω)
CaPr0	796 ± 1.8	55.04 ± 0.5	592 ± 1.5	1.65 ± 0.06	46.8	0.152
Ca1Pr0125	742 ± 1.7	56.35 ± 0.5	556 ± 1.4	1.47 ± 0.05	92.9	0.118
Ca1Pr025	759 ± 1.7	58.76 ± 0.7	569 ± 1.4	1.67 ± 0.06	131.3	0.133
Ca1Pr05	666 ± 1.6	41.22 ± 0.4	499 ± 1.2	8.49 ± 0.2	22.05	0.075

Summary of Section 3.6: The addition of Pr_6O_{11} significantly influences on the microstructure and electrical properties of ZnO-Bi-Ca varistors by tailoring the grain size and grain boundary characteristics. At an optimal content (~0.25% mol), the material exhibits a relatively uniform microstructure, enhanced grain boundary potential barrier height, and improved nonlinearity. This reduces the leakage current and enhance the current-blocking capability in the low-electric-field region.

3.7. Characterization of optimized CaO-doped nano-ZnO surge arrester varistors and impulse current testing of standard varistors

3.7.1. Morphological and structural characteristics

The post-sintered ZnO microstructure consists of fairly uniform polyhedral grains with clear grain boundaries. The grain size is mainly distributed in the range of 2 – 4 μm, centered about 3 μm, which reflects a relatively uniform grain growth process. The uniform microstructure helps maintain grain boundary network and the form a continuous Schottky potential barriers.

3.7.3. Current–Voltage characteristics

The varistors exhibit high stability, with a breakdown electric field E_{1mA} ≈ 694.7 V/mm, threshold voltage U_s ≈ 521 V/mm, and low leakage current density (~1.39 µA/cm^2), reflecting a relatively uniform grain boundary structure. The nonlinearity coefficient is relatively high, ranging between 52 and 54 (Table 3.19).

Table 3.19. DC electrical properties of ZnO-Bi-Ca varistors fabricated from spray-dried powder

Sample	E_{1mA} (V/mm)	α	E_s (V/mm)	U_c (V/mm)	J_L (µA/cm^2)
MOV.SP02(11)	693.8	52.4	520.3	333.4	1.37
MOV.SP03(16)	694.9	52.9	521.1	318.4	1.46
MOV.SP04(C)	695.2	53.2	520.7	318.0	1.32
MOV.SP05(D)	694.7	53.8	521.6	338.5	1.41
MOV.SP06(E)	695.0	53.4	521.4	337.8	1.39
Average	694.7 ± 0.4	53.1 ± 0.4	521.0	329.2 ± 8.8	1.39 ± 0.04

3.7.4. Complex impedance

The Cole-Cole plot exhibits an equivalent circuit model of R_o in series with (R_{gb}//C_{gb}) network (Figure 3.51a), with R_{gb} ≈ 309.9 MΩ (corresponding to a grain boundary resistivity of 61.3 MΩ.m) and R_o ≈ 1.73 Ω. This confirms that the grain boundaries strongly govern the electrical conduction mechanism of the material. The resistivity decreases with frequency from ~10^7 - 10^8 Ω.m down to ~10^{-1} Ω.m, demonstrating that the spray-drying process effectively enhances grain bonding and nonlinear electrical conductivity (Figure 3.51b).

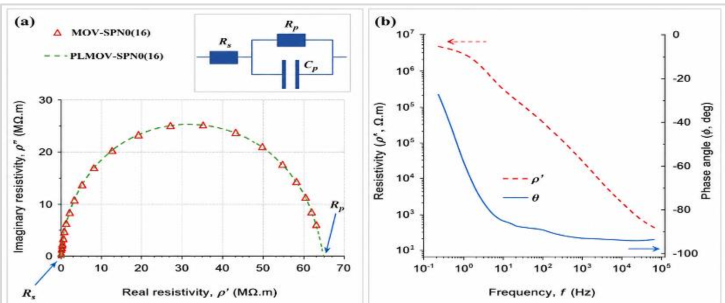

Figure 3.51. (a) Cole-Cole plot of AC resistivity and (b) AC resistivity as a function of frequency of a representative varistors.

3.7.5. Impulse voltage properties

Under 8/20 µs current impulse testing, the residual voltage of the ZnO–Bi–Ca varistors increases with rising impulse current amplitude, reaching U_{5kA} = 20.43 ± 0.5 kV và U_{10kA} = 20 ± 1 kV, reflecting the overvoltage withstand capability of the material. Furthermore, the residual voltage ratio (commonly designated as the clamping ratio, K_r), represents one of the most important technical parameters for evaluating the protective performance of varistors. The measured ratio $K_r = U_{du}/U_{1mA}$ = 2.0 - 2.2, fully satisfies the overvoltage protection requirements of the varistors (Table 3.20).

Table 3.20. (8/20 µs) impulse voltage characteristics of ZnO–Bi–Ca varistors used for surge arrester fabrication

TT	**Sample**	**U_{5kA} (kV)**	**U_{10kA} (kV)**	**U_{J1mA} (kV)**	**U_{5k}/U_{J1mA}**	**U_{10k}/U_{J1mA}**
1	MOV.SP02(11)	21.44	22.59	10.5	2.04	2.15
2	MOV.SP03(16)	17.94	19.33	9.0	1.99	2.15
3	MOV.SP04(C)	17.27	19.37	9.05	1.91	2.14
4	MOV.SP05(D)	17.88	19.58	8.59	2.08	2.28
5	MOV.SP06(E)	17.52	19.14	8.31	2.11	2.30
	Average	18.4±1.2	20 ± 1	9.1 ± 0.6	2.0 ± 0.1	2.2 ± 0.1

Summary of Section 3.7: The fabrication process integrating spray-drying with sintering enables the production of uniform precursor powders, thereby significantly enhancing the microstructural uniformity of the material. Consequently, the obtained material exhibits high densification, stable grain boundary attice, and consistent mechanical and electrical properties, with a breakdown electric field E_{1mA} approx 695 V/mm, nonlinearity coefficient > 54, a low leakage current density, and a residual voltage ratio K_r > 2 under impulse current levels of 5 kA and 10kA. The results confirm that this method is effective in optimizing the microstructure and enhancing the characteristics of ZnO varistors for surge arrester applications.

CONCLUSIONS

This thesis has established an optimized fabrication process for varistors based on nano-ZnO doped with CaO and Pr_6O_{11}. The important scientific and practical contributions of this research are summarized as follows:

1. A electrode area correction method was proposed to eliminate systematic errors in electrical characterization. The method demonstrates high linearity between varistor voltage and sample thickness (with correlation coefficients R^2 reaching 0.9997 - 0.9998), contributing significantly to the precision of materials research.
2. The optimal technological conditions were identified at a compacting pressure of 75 - 100 MPa and a sintering temperature of 1050 ^oC for 2h. The fabricated material has a uniform microstructure, high grain boundary density, and a threshold electric field $E_s \approx 739.6$ V/mm.
3. Experimental results indicate that the nano-ZnO-based varistors significantly enhances overvoltage protection performance compared to traditional micro-ZnO varistors, achieving a 25 - 33% increase in breakdown electric field and threshold voltage. This demonstrates that grain size control and grain boundary density enhancement are key methods to enhance the threshold electric field and electrical properties of varistors.
4. Mixing1 % mol CaO and 0.25 % mol Pr_6O_{11} produced varistors with a high nonlinearity coefficient and a threshold electric field 1.2 times higher than that of micro-ZnO varistors. This result confirms the effectiveness of adding CaO and Pr_6O_{11} in appropriate amounts to controls the grain boundary potential barrier height and enhance the threshold electric field.
5. The spray-drying technology yielded materials with high cohesive strength, uniform ZnO grain size (2 – 4 µm), high threshold electric field, and high-voltage impulse current capability, opening up significant potential for developing domestic ZnO varistor materials for surge arrester manufacturing.

LIST OF PUBLICATIONS DERIVED FROM THE DISSERTATION

1. **Huy Nguyen Trung**, Trang Nguyen Van, Kieu Anh Vo Thi, Hong Cao Thi, Xuyen Nguyen Thi, Tuan Anh Nguyen, Tuan Anh Nguyen, Lam Tran Dai, Chinh Tran Van, Duy Lai Van, Duong La Duc and Tham Do Quang. "Tailoring morphological and electrical properties of nanoplate-ZnO varistors via sintering temperature". *RSC Adv.*, 2025,15, 20006-20019.
2. Do Quang Tham, **Nguyen Trung Huy**, Nguyen Tuan Hung, Nguyen Tuan Anh, Nguyen Dinh Anh Son, Nguyen Thi Xuyen, Pham Thi Nam, Vo Thi Kieu Anh, Nguyen Van Trang, Cao Thi Hong, Nguyen Thi Thu Trang, Tran Dai Lam, "Electrode area correction in the evaluation of DC electrical properties of ZnO-based varistors". Vietnam Journal of Science and Technology. https://doi.org/10.15625/2525-2518/23429.
3. **Nguyen Trung Huy**, Nguyen Tuan Hung, Nguyen Tuan Anh, Nguyen Thi Xuyen, Pham Thi Nam, Vo Thi Kieu Anh, Nguyen Van Trang, Cao Thi Hong, Nguyen Dinh Anh Son, Nguyen Thi Thu Trang, Do Quang Tham. “How effective electrode diameters affect on the electric properties of ZnO varistor”. The 9th National Chemistry Conference - Vietnamese Chemistry for Green Development, November 28–29, 2025, Hanoi University of Science and Technology, Hanoi, Vietnam.
4. **Nguyen Trung Huy**, Vo Thi Kieu Anh, Cao Thị Hong , Nguyen Thi Xuyen , Pham Thi Nam, Do Quang Tham “Tối ưu hóa quá trình thiêu kết nhằm cải thiện vi cấu trúc và đặc tính điện của varistor trên nền ZnO - Pr”. The 14th National Conference on Solid State Physics and Materials Science - SPMS 2025, November 5–7, 2025, Dak Lak, Vietnam.